AJNR

Assessment of carotid artery stenosis by MR angiography: comparison with x-ray angiography and color-coded Doppler ultrasound.

C M Anderson, D Saloner, R E Lee, V J Griswold, L G Shapeero, J H Rapp, S Nagarkar, X Pan and G A Gooding

AJNR Am J Neuroradiol 1992, 13 (3) 989-1003
http://www.ajnr.org/content/13/3/989

Assessment of Carotid Artery Stenosis by MR Angiography: Comparison with X-ray Angiography and Color-Coded Doppler Ultrasound

Charles M. Anderson,[1,2] David Saloner,[1,2] Ralph E. Lee,[1,2] Virginia J. Griswold,[1,2] Lorraine G. Shapeero,[2] Joseph H. Rapp,[3] Sumant Nagarkar,[1] Xianmang Pan,[3] and Gretchen A. W. Gooding[1,2]

Purpose: To compare magnetic resonance angiography (MRA) with duplex Doppler ultrasound (US) and x-ray angiography (XRA) in the evaluation of the carotid bifurcation. **Methods:** The carotid arteries of 61 patients were studied using MRA, US, or XRA; 31 of the patients underwent all three examinations. MRA included both 2D and 3D time-of-flight sequences. Internal and external carotid artery origins were graded normal, mild, moderate, severe, or critical stenosis, or complete occlusion by each of the three studies. **Results:** Spearman rank correlations of both internal and external carotid artery grades were 0.85 (MRA and XRA), 0.69 (MRA and US), and 0.73 (XRA and US). For internal carotid artery origins only, the correlations were 0.94 (MRA and XRA), 0.85 (MRA and US), and 0.82 (XRA and US). Of discrepancies in internal carotid artery interpretation greater than one grade, seven resulted from US error, three from MRA error, and one from XRA error. A 2-cm partially thrombosed aneurysm detected by US and MRA was missed by XRA. Of 16 possible ulcers on XRA, 11 were noted by MRA, none by US. **Conclusions:** MRA and XRA are similar in assessment of carotid bifurcation stenosis. MRA, like US, permits direct visualization of plaque. This preliminary study suggests that MRA may be used to clarify equivocal findings of US, or replace XRA in presurgical planning.

Index terms: Arteries, carotid; Arteries, stenosis and occlusion; Magnetic resonance angiography (MRA); Ultrasound, Doppler

AJNR 13:989–1003, May/June 1992

The carotid artery is among the first vessels to be investigated by magnetic resonance angiography (MRA) because of the clinical interest in predicting and preventing stroke. Rapid and laminar blood flow in the normal carotid artery is well suited to MRA, particularly by the so called time-of-flight (TOF) principle imaging (1) (also called "flow-related enhancement" or simply "inflow"). MR imaging coils are available for the neck with adequate sensitivity for high-resolution images, permitting visualization of relatively small vessels. The quality of carotid MR angiograms has improved dramatically over the past year (2) due to the use of very short echo times and small voxel volumes to minimize turbulent flow signal loss (3).

Until recently, investigations of carotid artery imaging have revolved around technical issues such as the selection of three-dimensional (3D) (1) or two-dimensional (2D) (4) Fourier techniques. In its 3D implementation, a slab of data is acquired that offers equally high resolution and sensitivity to flow in any direction, but exhibits poor contrast in slow velocity situations. This is the result of saturation of blood as it travels through the slab. 2D TOF angiograms are acquired as a series of thin transverse slices that are sensitive even to highly compromised flow, but which provide lower resolution and suffer from in-plane saturation, which is the loss of contrast when vessels travel parallel to the slices.

Received June 4, 1991; accepted and revision requested August 21; revision received October 3.

[1] Department of Radiology (114), San Francisco Veterans Administration Medical Center, 4150 Clement Street, San Francisco CA 94121. Address reprint requests to C. M. Anderson.

[2] Department of Radiology, University of California, San Francisco, School of Medicine, Third and Parnassus, San Francisco, CA 94143.

[3] Departments of Surgery, San Francisco Veterans Administration Medical Center and University of California, San Francisco.

AJNR 13:989–1003, May/June 1992 0195-6108/92/1303-0989

Although the technical factors of TOF angiography of the carotid are becoming better understood, the clinical advantages of MR over the established procedures of duplex Doppler ultrasound (US) and conventional x-ray angiography (XRA) are only now being addressed (5–7). Early studies have employed either 2D or 3D techniques, but not both. Some problems encountered by these investigators related to their choice of technique. For example both Litt et al (5) and Kido et al (6), using 2D TOF, were occasionally unable to differentiate the internal (ICA) and external (ECA) carotid arteries because they could not visualize branches of the ECA. This problem could have been avoided by the use of a 3D acquisition, which typically does visualize ECA branches. Masaryk et al (7), using 3D TOF, noted that occasionally portions of the carotid were not seen because they extended to one side of the slab. These segments could have been detected in the transverse slices of a 2D acquisition.

In the current investigation, we avoid the issue of 2D versus 3D TOF angiography by acquiring both sequences and taking advantage of the strengths of both methods. MRA is compared to US and XRA in order to assess the agreement among these modalities in the evaluation of the carotid bifurcation.

Methods

Patient Population

Fifty-eight male and three female patients ages 48 to 84 with a high clinical suspicion for stenotic carotid artery disease were imaged by MRA. Of these, 53 also underwent US, and 34 underwent XRA. Thirty-one patients had all three modalities. Of the XRA patients, eight had unilateral studies only. The MRAs of two patients were interpreted on one side only because of the presence of surgical clips that distorted the images. Two MRAs were analyzed on one side only because the patient underwent endarterectomy between the XRA examination and the MRA. This left a total of 50 carotid bifurcations by all three modalities, 61 by MRA and XRA, 93 by MRA and US, and 50 by XRA and US.

Six patients who failed MRA were not included in this comparison. Three had excessive head motion, two had bilateral surgical clips, and one had a tortuous carotid artery that was not contained in the imaging volume.

MRA Studies

MRA exams were performed on a 1.5-T Magnetom (Siemens AG, Erlangen, Germany) using either a linearly polarized transmit-receive head coil or a carotid imaging coil fabricated by the authors (Fig. 1). This second coil was similar in principle to a coil previously described (8). The coil was a two-turn loop, one anterior and one posterior to the neck. The posterior turn was smaller so that it could lie under the back. The turns were in series to force them to resonate at the same frequency despite their asymmetric shape. Distributed capacitance divided the loop into 10 equal lengths. The coil rested on a track that allowed it to be translated into position, typically so that the inferior edge of the coil was 10 cm caudal to the chin. The coil was then caudal enough to visualize the proximal CCA, but rostral enough to presaturate dural sinus blood in the occiput.

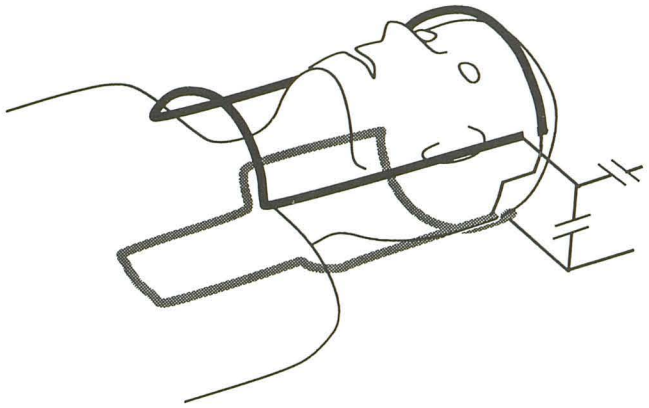

Fig. 1. Schematic diagram of carotid imaging coil used to acquire angiograms. Coil consists of two loops in series with posterior loop shaped so that it can rest beneath the shoulders. This permits placement of coil at lower neck and upper chest in order to visualize proximal CCA.

Twenty-four transverse sequential 2D TOF slices were acquired using fast low-angle shot (FLASH), 40/10/25° TR/TE/θ, slice thickness of 4 mm, acquisition time of 3.5 min, with velocity compensation in the slice and frequency-encoding direction, and with a coronal saturation band over the dural venous sinuses of the occiput to eliminate jugular vein signal. Using the transverse slices to localize the bifurcations, two sagittal 3D TOF slabs were prescribed, one centered on each bifurcation, using the method described by Masaryk et al (9). Fast imaging with steady-state precession (FISP) was acquired with 70/7–8/20–30° TR/TE/θ, 32 partitions per slab, a matrix of 256 × 256, field of view (FOV) of 220 mm, acquisition time of 9.6 min, and velocity compensation in frequency and slab selection directions. The long repetition time ensured very little saturation of blood over the imaging volume. Again, a coronal saturation band was placed over the occiput. In some cases, a second coronal saturation band was placed anterior to the carotid to remove artifact from tongue and jaw motion. In all but the first 17 patients in the series, a transverse 3D TOF slab was then acquired. The slab was positioned at the bifurcation unless a lesion away from the bifurcation was noted on the sagittal acquisition, in which case the slab was centered at the lesion (FISP, 50/7/25° TR/TE/θ, 64 partition, matrix = 192 × 256, FOV = 210, time = 10.3 min, superior transverse saturation band).

Maximum intensity projections (MIPs) (10) could be quickly calculated without transfer of data to a separate work station. This permitted inspection of the angiograms and execution of additional sequences, if necessary, before the patient left the magnet. Eleven orientations were calculated of an interactively selected small volume centered at each bifurcation. These projections were photographed, together with the individual slices from the transverse 2D acquisition and partitions through the bifurcations from the sagittal 3D acquisition. Because the 2D slices were acquired with relatively low resolution, they were rarely used to generate a MIP. In all, there were eight sheets of film per study.

XRA Studies

Twenty patients were investigated by digital subtraction angiography (DSA), and 14 patients by cut film. Common carotid artery (CCA) injections were made with imaging in two projections whenever possible. In five patients, arch injections only were performed.

US Studies

Color flow Doppler imaging was performed with a 7.5-MHz or 5-MHz transducer (Quantum Medical Systems Quad-1, Issaquah, WA). Carotids were examined in longitudinal and transverse plane, and recorded on Polaroid film and video tape. The Doppler angle was maintained at approximately 60° or less to the course of the vessel. Spectral analysis was performed on areas of flow abnormality, or, if none existed, at the region of the maximum velocity of the CCA, ICA, and ECA. Peak systolic and end diastolic velocities and ICA/CCA velocity ratios were recorded.

Assignment of Stenosis Grade

Diameter percent stenosis grades are defined in Table 1. MRA and XRA grades were assigned by comparing the observed width of the stenotic vessel with the width of the closest normal portion of vessel. The orientation that demonstrated the greatest stenosis was chosen. When the stenosis extended over a long segment so that there was no immediately adjacent normal segment for comparison, the normal diameter was estimated by reference to the shape of the bifurcation on the contralateral side, or to a diagram of an average carotid bifurcation. When interpreting MR angiograms, estimation of the normal size of the vessel segment was facilitated by viewing individual partitions of a 3D acquisition. On these images, the muscular wall of the vessel could be seen directly. The MRA and XRA studies were placed in random order, so it was not possible to correlate the two. Images were read in blinded fashion by a panel of three readers. The readers each had 2 or more years experience in interpreting MRA, and were familiar with common artifacts such as saturation, turbulence, flow separation, and MIP effects (11). A vote was taken for each study, from which a majority grade assignment was made. Only the proximal 4 cm of the ICA and ECA were graded. Stenoses at other sites were ignored so that correlation could be made with US.

TABLE 1: Stenosis grade definitions for percent diameter stenosis in the proximal ICA and ECA

	XRA, MRA	US
Normal	0	0
Mild	1–39	1–39
Moderate	40–59	40–59
Severe	60–94	60–79
Critical	95–99	80–99
Complete	100	100

Doppler cross-sectional diameter stenosis was assigned on the basis of the measured velocities according to the algorithm recommended by Bluth et al (12).

Statistical Comparisons

A measure of agreement between the modalities for stenosis grades was computed using the Spearman rank correlation (13). Correlation was made between all available pair-wise data, and again for the subset of vessels for which there were data from all three modalities.

A Pearson correlation was calculated between the stenosis grades. Unlike the Spearman test that considers only the hierarchy of stenosis categories, the Pearson test compares the relative magnitude of the stenosis. Magnitudes were approximated by assigning the median of the category range to that category. For example, all moderates were assigned a value of 0.5. Vessels critical by US were assigned 0.9, while critical MRA and XRA were assigned 0.975. The assigned stenosis values were also used to compute a mean percent stenosis for each modality.

Inter-Reader Variability

A test was made of the variability of interpretation of angiograms by different readers. Forty-eight carotid x-ray angiograms were shown to four readers, who arrived at independent grades of the proximal ICA and ECA vessels. If any of the four readers felt a study was technically less than optimal, it was removed. Spearman correlations were computed between the four sets of interpretations of the 40 remaining studies.

Results

MRA Failures

The most common reason for failure of MRA was patient motion. This was particularly a problem in patients who had a prior stroke and who exhibited involuntary motion, as well as in patients with cervical spine disease and paresthesias. These patients were not included in the analysis. Surgical clips were also problematic,

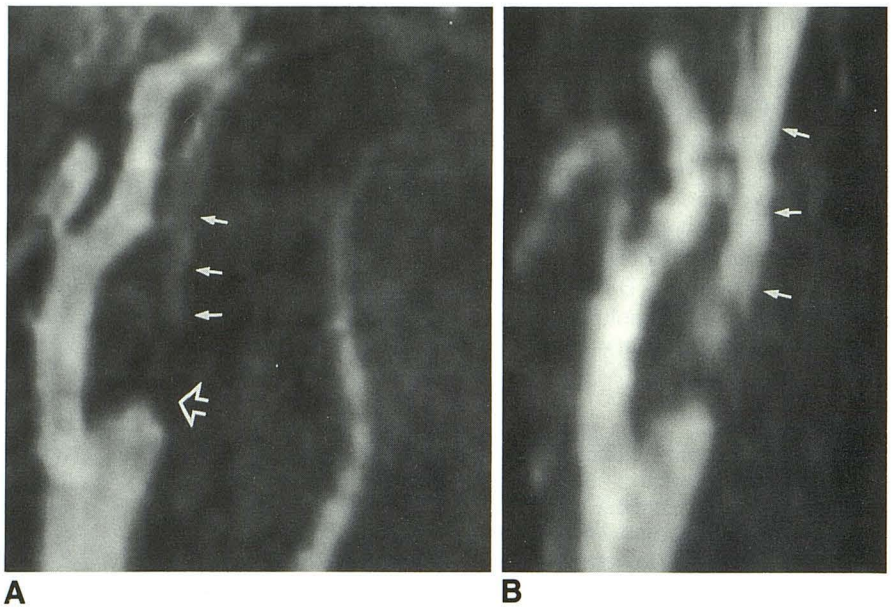

Fig. 2. Comparison of 2D TOF and 3D TOF MRA of critical stenosis of proximal ICA demonstrating advantage of 2D in slow flow conditions.

A, 3D TOF MRA. ICA (*small arrows*) is weakly visible beyond stenosis. At stenosis (*open arrow*) there is loss of signal.

B, Sequential 2D TOF MRA more accurately depicts the caliber of the ICA (*small arrows*) beyond the stenosis. 2D TOF images are advantageous in discriminating critical stenoses from complete occlusions.

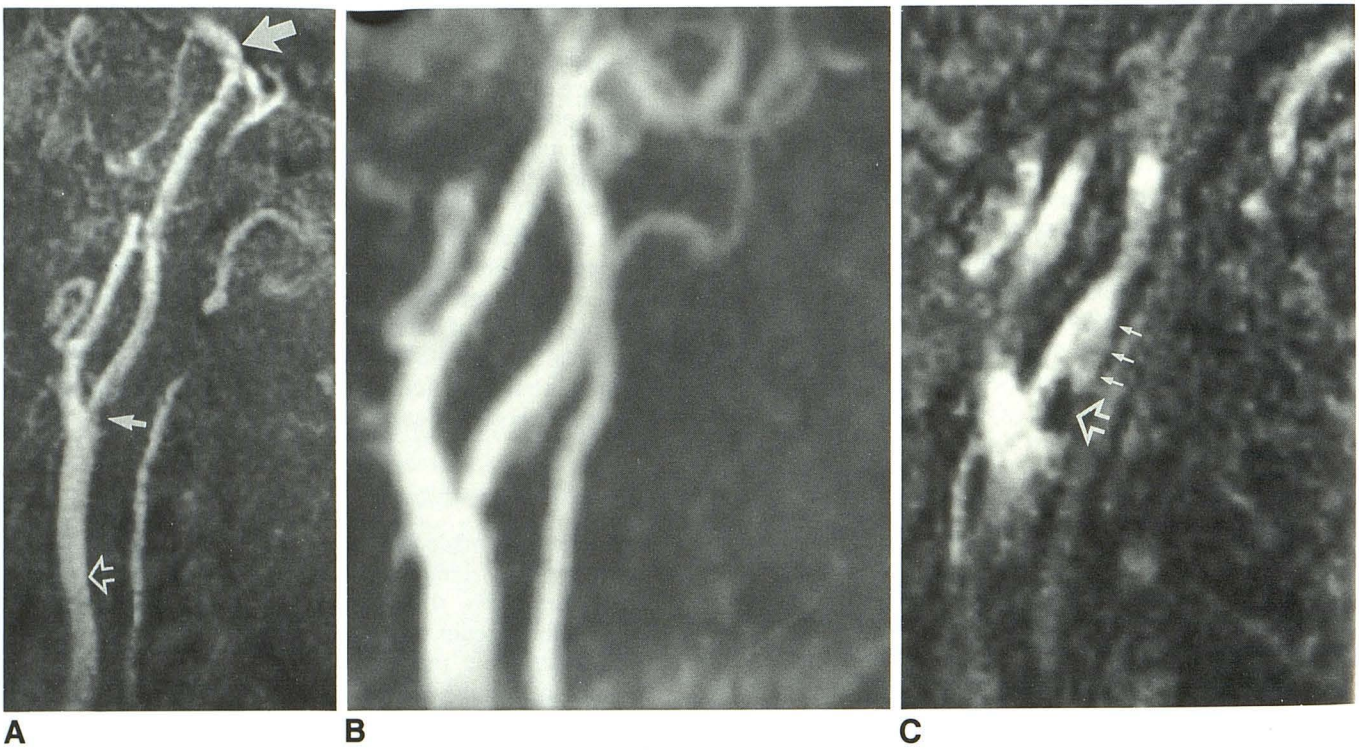

Fig. 3. Visualization of plaque on single partitions.

A, Sagittal 3D TOF MRA depicts carotid from proximal CCA (*open arrow*) to petrous angle of ICA (*large arrow*). Severe stenosis noted of proximal ICA (*small arrow*).

B, Transverse 3D TOF MRA of stenosis demonstrates greater background suppression and stronger contrast than does sagittal acquisition.

C, Single partition of 3D TOF MRA through dark plaque (*open arrow*) in lumen of proximal ICA. Wall of vessel is visible as black line (*small arrows*).

particularly in that they could not be recognized on MIPs, where they could simulate a stenosis. Clips could be readily detected on individual slices by the presence of the familiar round dark-field artifact.

A marked difference in quality was noted between the earliest MRA studies and those collected later in the series. This improvement resulted from better head motion restraint, the choice of smaller voxel sizes (partition width of

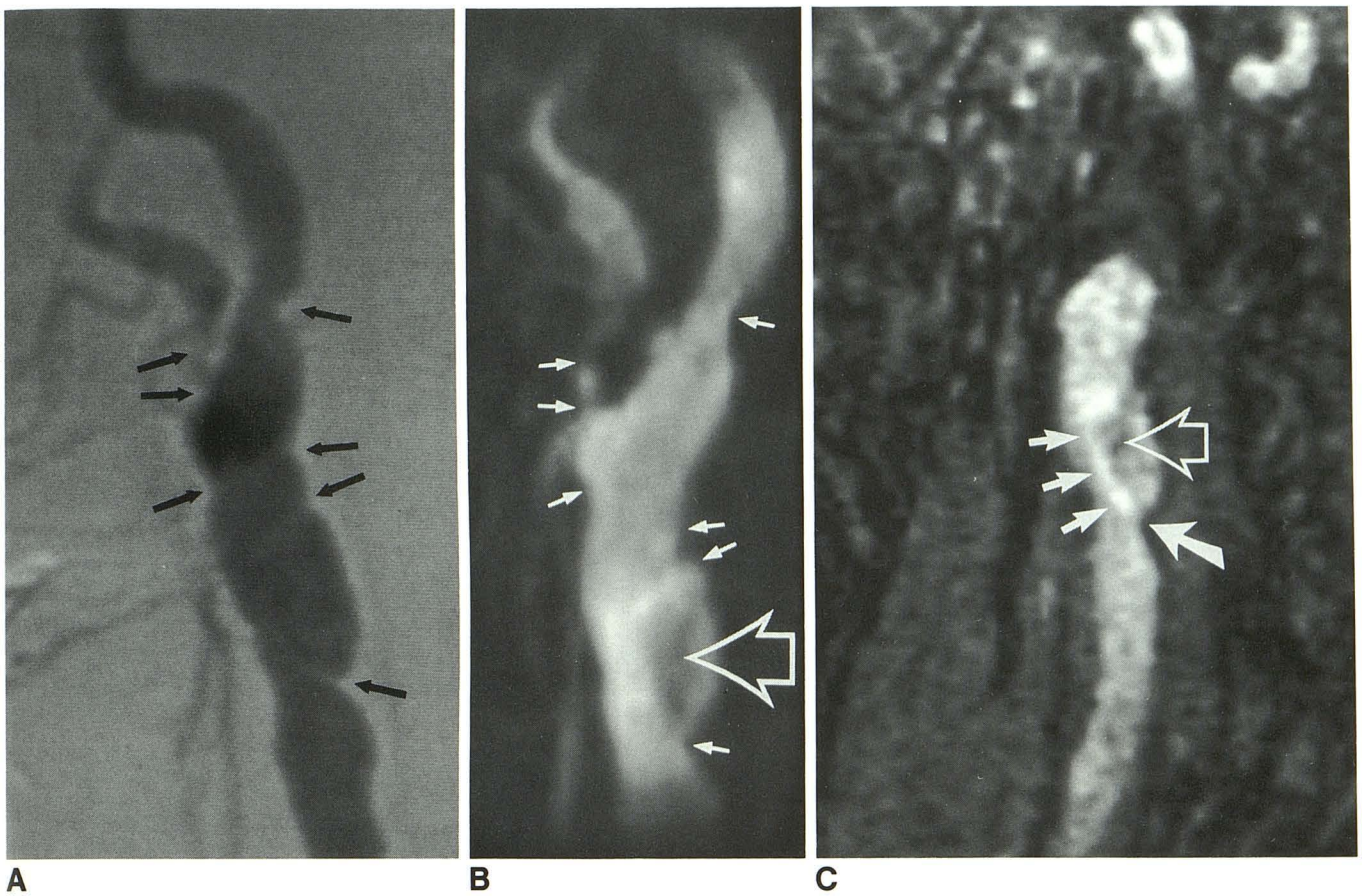

Fig. 4. Visualization of flow patterns on single partitions.

A, XRA of bifurcation showing complex pattern of stenoses (*arrows*).

B, MRA from transverse 3D TOF acquisition shows same stenoses (*closed arrows*). A portion of the distal common carotid artery has decreased intensity suggestive of thrombus (*open arrow*).

C, Inspection of each of the sagittal 3D TOF partitions through the CCA shows there is no thrombus in area of low signal. Instead, a focal plaque on posterior wall of CCA (*large closed arrow*) anteriorly deflects the stream of blood (*small arrows*), leading to flow separation and reverse flow above plaque (*open arrow*). This interpretation was confirmed by late image from XRA contrast injection series that showed delayed clearing of this site with nonopacified blood.

1.0 mm vs 1.5 mm for the earliest studies), improved software that allowed more flexibility in slab positioning, and the construction of a dedicated carotid imaging coil.

Assignment of MRA Stenosis Grade

In arriving at a carotid stenosis grade by MRA, all available images were used including transverse sequential 2D TOF, which were viewed as individual slices, sagittal 3D TOF, which were viewed as single partitions and as MIPs, and transverse 3D TOF MIPs. The transverse 2D images were sensitive to slow flow, and could be used to differentiate critical stenoses from occlusions (Fig. 2). They also provided a cross-sectional image of the vessel that aided in determining percent diameter stenosis. They were viewed as individual slices and were rarely processed into MIPs. Single images from 3D sagittal acquisitions were useful in direct visualization of plaque (Fig. 3), in understanding anatomy in three-dimensions, in revealing flow patterns (Fig. 4), and in visualizing features that might be lost in the MIP process (Fig. 5) (11). The MIP of the sagittal 3D data provided a large FOV image with little distal saturation. The ICA could be seen from near its origin up to the petrous angle. This relative immunity to saturation resulted from the small flip angle of 25° and long TR of 70 msec. Transverse 3D TOF MIPs provided stronger contrast than did sagittal 3D TOF MIPs, but displayed a shorter segment of the vessel. They were generally preferred for visualizing ulcers (Figs. 6 and 7) and other small features. 3D TOF MRA was preferable to 2D TOF in visualization of tortuous and transversely oriented vessels. These vessels became saturated in 2D acquisition (Fig. 8).

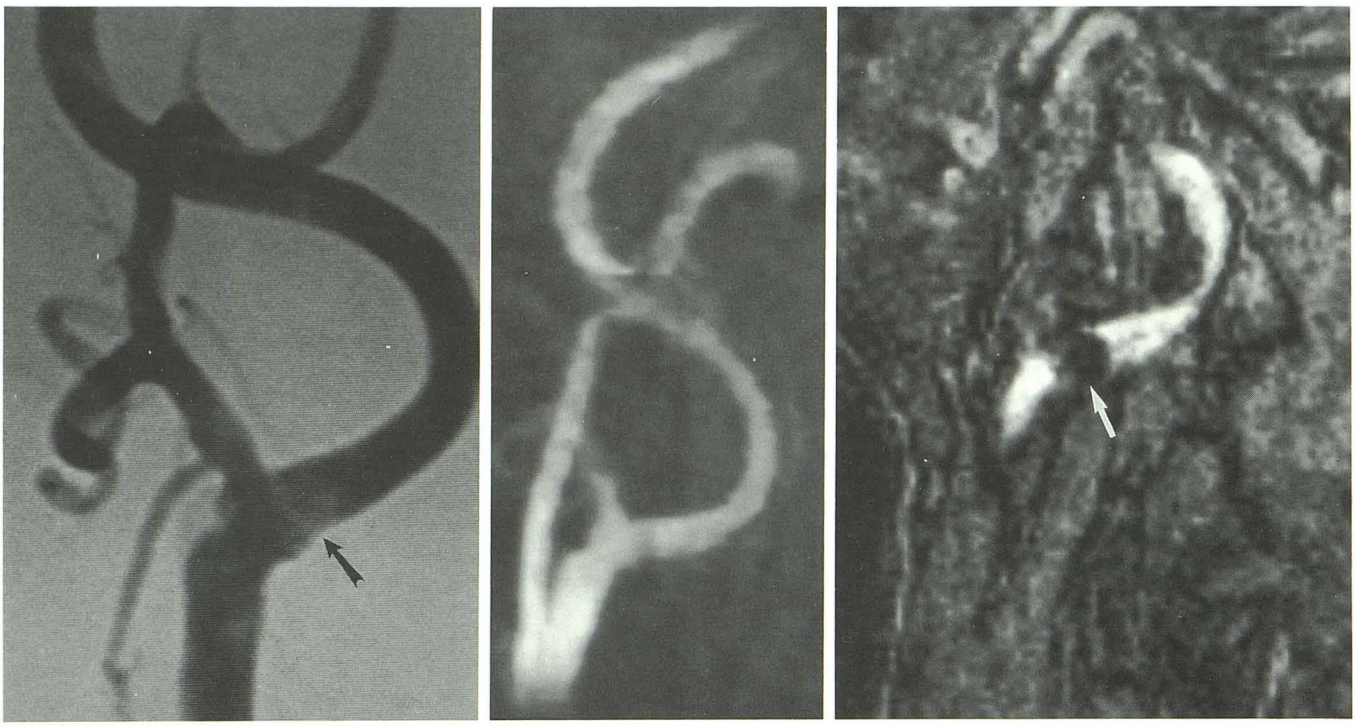

Fig. 5. Importance of inspecting single partitions in plaque detection.

A, XRA of carotid bifurcation shows lower density at carotid bifurcation (*arrow*). This is indirect evidence of plaque on anterior or posterior wall leading to narrowing of vessel. XRA transmission image depicts an integral of the contrast projected through the vessel.

B, MRA of carotid appears normal on MIP. MIP differs from XRA in that it displays the highest intensity pixel in the projection of the vessel rather than an integral of pixel intensities. Plaque en face may be missed on MIP.

C, Plaque (*arrow*) clearly seen on individual partition of set used to calculate MIP. For most accurate evaluation of stenosis, individual partitions through vessel should be photographed and interpreted with the MIP.

Fig. 6. Detection of ulcer by MRA.

A, XRA shows shallow ulcer of bulb (*arrow*) in proximal ICA.

B, This ulcer well depicted on transverse 3D TOF MRA (*arrow*).

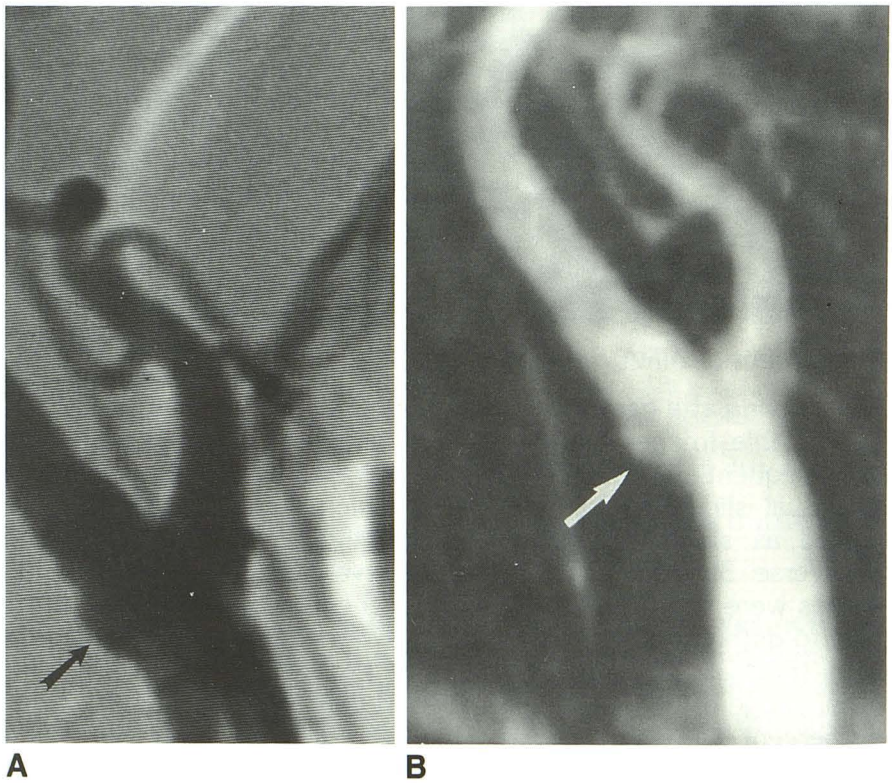

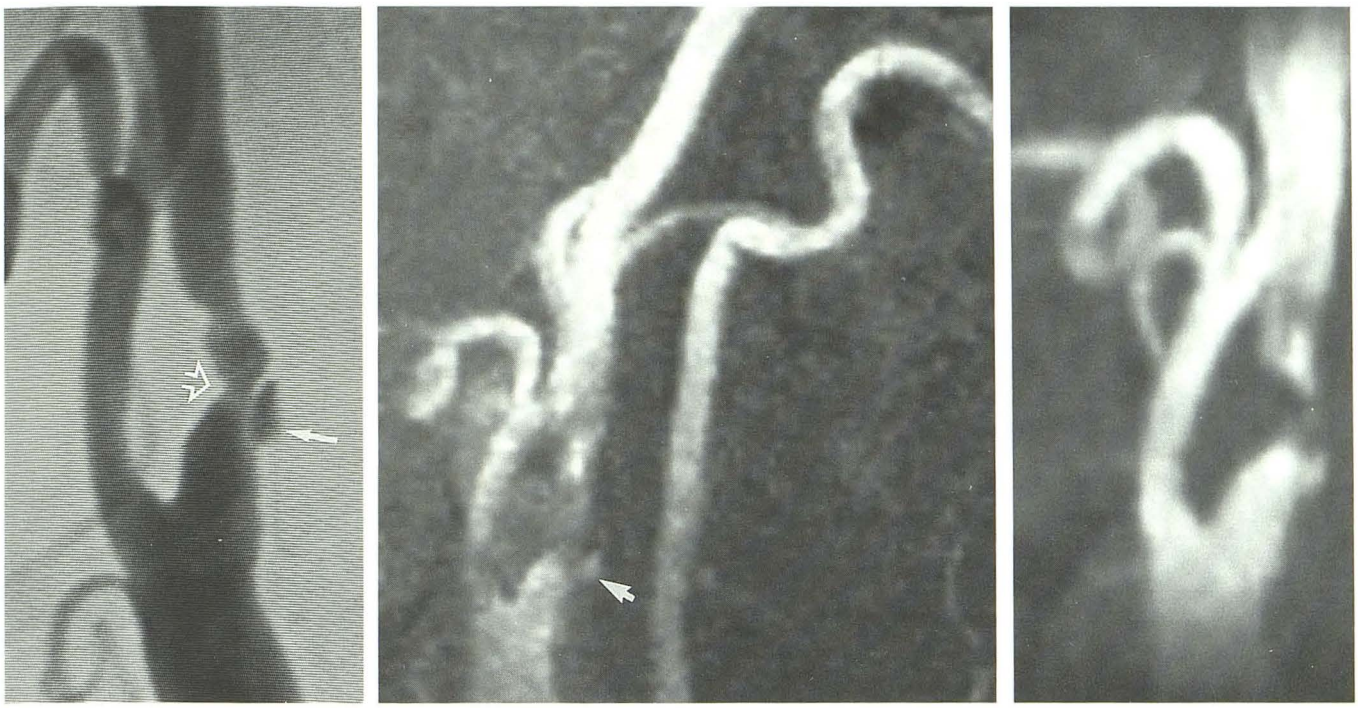

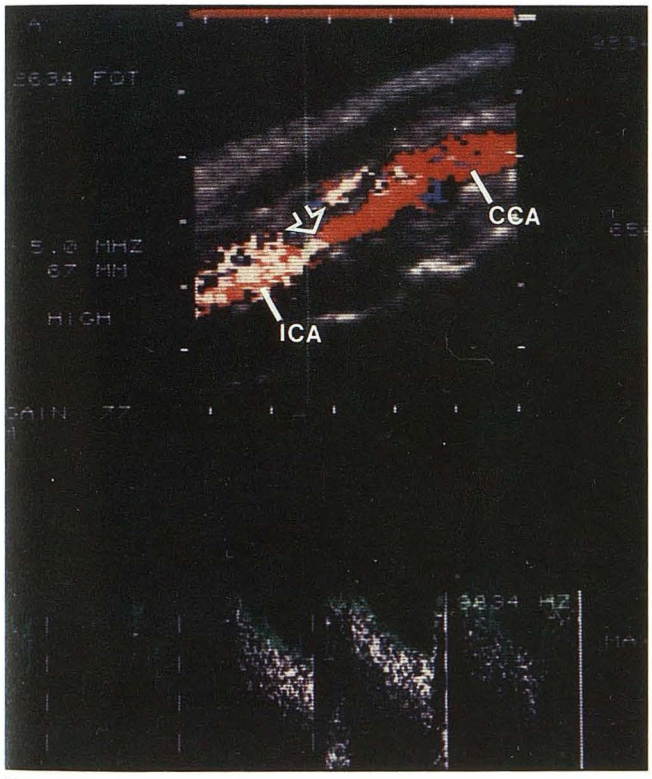

Fig. 7. Detection of ulcer by MRA.

A, XRA shows ulcer of proximal ICA (*closed arrow*), near severe stenosis (*open arrow*).

B, Sagittal 3D TOF MRA. Stenosis is overestimated as critical due to turbulent signal loss. (Ulcer = arrow).

C, Transverse 3D TOF MRA. Vessel depicted with greater contrast.

D, Longitudinal color-coded Doppler sonogram. Severe stenosis (*open arrow*) is noted evidenced by spectral broadening and elevated velocity. Ulcer is not seen.

Use of three acquisitions together permitted an internal consistency check of any suspected lesion, thereby minimizing the possibility of a flow artifact being mistaken for a stenosis. When two images disagreed, the less stenotic appearing image was selected.

Tests of Agreement

Statistical results are summarized in Table 2. The degree of correlation between all three modalities was very strong. For each of the 15 pairwise correlations listed, the *P*-value was less than

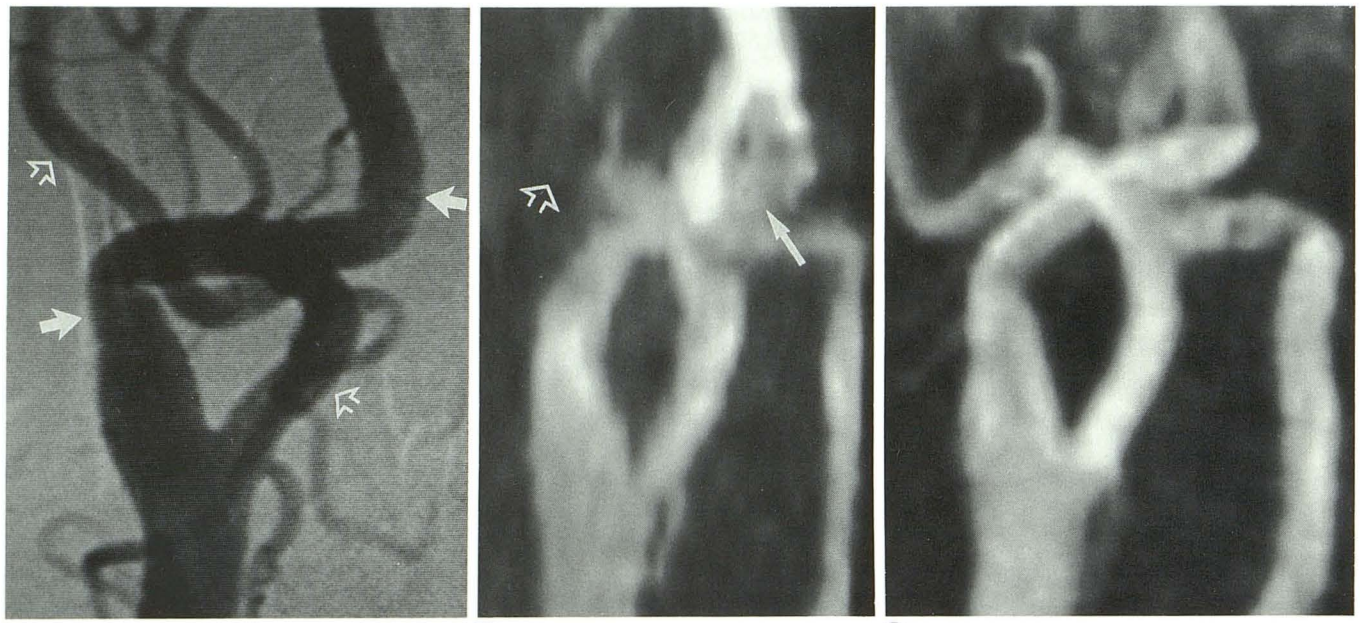

Fig. 8. Comparison of 2D TOF and 3D TOF MRA in tortuous carotid vessels demonstrating advantage of 3D in visualizing transverse course of vessel.

A, XRA showing crossing of transversely oriented ICA (*closed arrows*) and ECA (*open arrows*).

B, 2D TOF MRA. Vessels are saturated in transverse segments leading to loss of contrast (*arrows*).

C, 3D TOF MRA. Contrast is independent of direction of vessel. Transverse segments well seen.

TABLE 2: Correlation coefficients for carotid imaging modalities

Test	Vessels	Patients[a]	MRA vs XRA	MRA vs US	XRA vs US
Spearman rank r	ICA and ECA	All	0.852 (122)	0.694 (186)	0.726 (100)
Spearman rank r	ICA and ECA	Three modality	0.868 (100)	0.697 (100)	0.726 (100)
Spearman rank r	ICA	All	0.938 (61)	0.854 (93)	0.820 (50)
Spearman rank r	ICA	Three modality	0.939 (50)	0.814 (50)	0.820 (50)
Pearson r	ICA	Three modality	0.943 (50)	0.785 (50)	0.808 (50)

Note.—All coefficients corrected for ties in rank. *P*-value of each correlation is less than .0001. Number of vessels compared in parentheses.

[a] Coefficients computed for all patients who underwent at least two modalities, and for only those which underwent all three modalities.

.0001. Correlation coefficients between XRA and MRA were larger than those between either of those modalities and US.

There are two potential deficiencies in the Spearman correlations. First, the definitions of stenosis grade differ slightly among US, MRA, and XRA. Specifically, critical is defined as 80%–99% by US and as 95%–99% by MRA and XRA. Second, information is discarded when performing nonparametric rank correlations rather than continuous variable correlations. For example, when comparing mild and severe, we know not only the relative rank (severe is greater, moderate is greater than mild) but also a quantitative relationship of stenosis (60%–94% is greater than 1%–39%). To compare the modalities on the basis of percent stenosis rather than stenosis grades, each vessel was assigned a percent stenosis based on the median of its category (eg, US critical was assigned to 90%), and a Pearson correlation was computed. The conclusion that MRA and XRA were more similar to each other than to US is unchanged by this statistic (Table 2).

Table 3 displays the stenosis assignments for each of the pair-wise comparisons. This table includes ICA data only. MRA and XRA show no assignments that are more than one grade different. If we assume that only those lesions that are severe or critical will result in surgery, only three cases (5%) might make a discrepant treatment recommendation. This number is small when one considers the fact that in practice different readers might make as many variations in assignment

TABLE 3: Comparison of ICA stenosis grades assigned by each modality

MRA Grade

XRA Grade	Nl	Mild	Mod	Sev	Crit	Occ
Nl	5	5				
Mild	1	6	6			
Mod			7	1		
Sev			2	3	6	
Crit				1	13	
Occ						5

MRA Grade

US Grade	Nl	Mild	Mod	Sev	Crit	Occ
Nl	13	19	1	1		
Mild	1	2	2			
Mod		2	1		2	
Sev	1	3	6	6	6	
Crit			2	1	16	
Occ						8

XRA Grade

US Grade	Nl	Mild	Mod	Sev	Crit	Occ
Nl	6	4			1	
Mild	2	2	1			
Mod				2		
Sev		3	4	4	3	
Crit				5	8	
Occ						5

Note.—Assuming that only severe and critical stenoses will result in endarterectomy, points that fall outside of the boxes with bold borders disagree as to whether surgery is recommended.

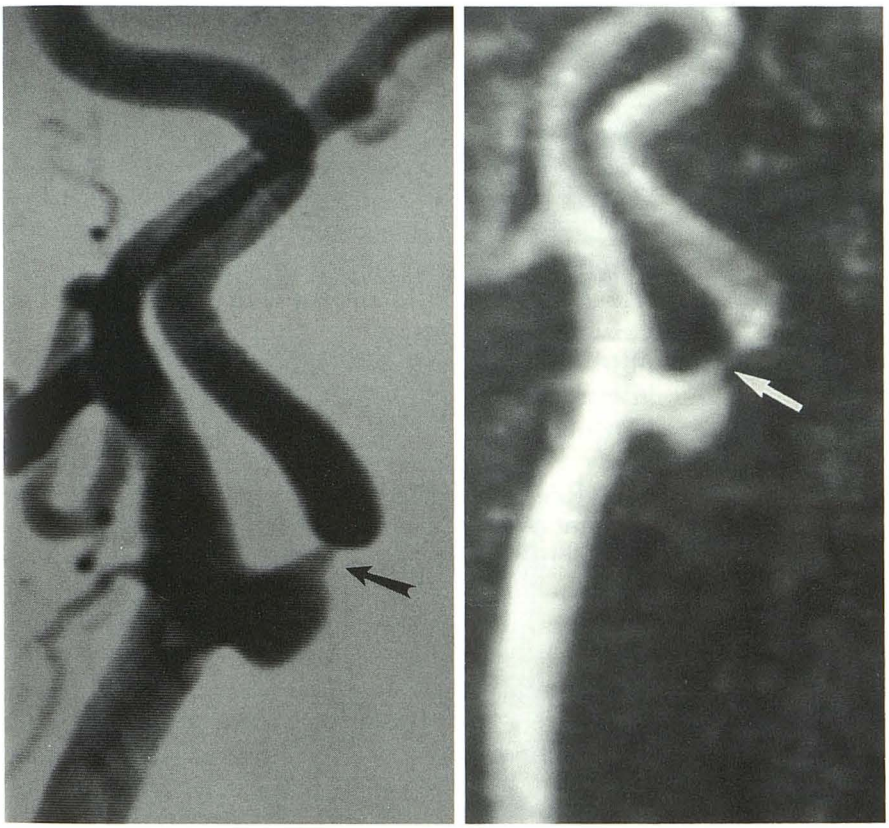

Fig. 9. Critical stenosis by MRA with lumen string sign.

A, Critical stenosis of ICA (*arrow*) on XRA.

B, Lumen is narrowed to string (*arrow*) on sagittal 3D TOF MRA.

on the basis of personal preference, particularly when a lesion falls near the boundary between two grades. An important observation is that there are no cases in which critical stenoses were mistaken for occlusions.

When XRA and US are compared, there are four cases with more than one grade difference, and 10 cases (20%) in which a different recommendation might be made with respect to surgical treatment.

Differences in Stenosis Grade

The mean diameter percent stenosis grades of the three modalities were found to be nearly identical. For ICAs and ECAs, the means were 59.2 (XRA), 63.7 (MRA), and 57.0 (US), while, for ICAs, only the means were 35.0 (XRA), 35.5 (MRA), and 37.6 (US). Inspection of Table 3 shows that when MRA and XRA disagreed, MRA often overestimated the stenosis by one grade.

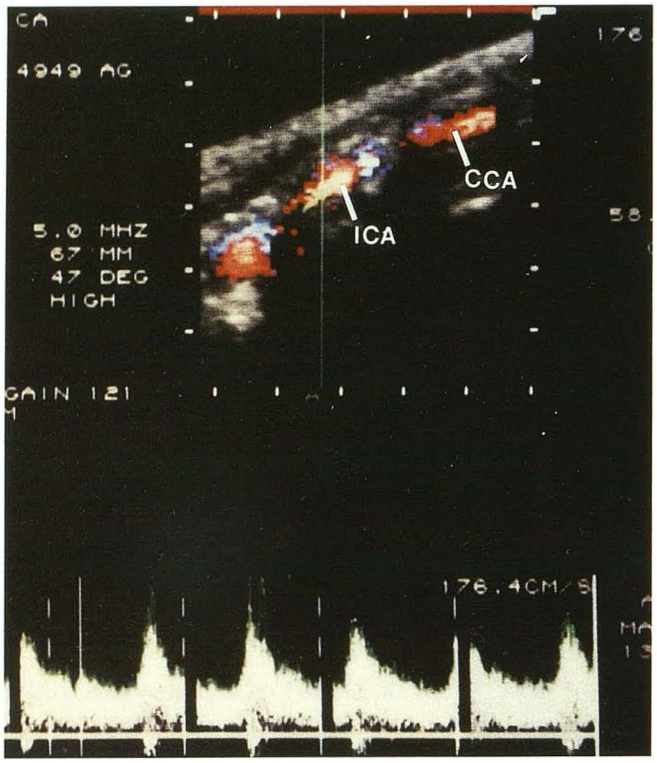

A

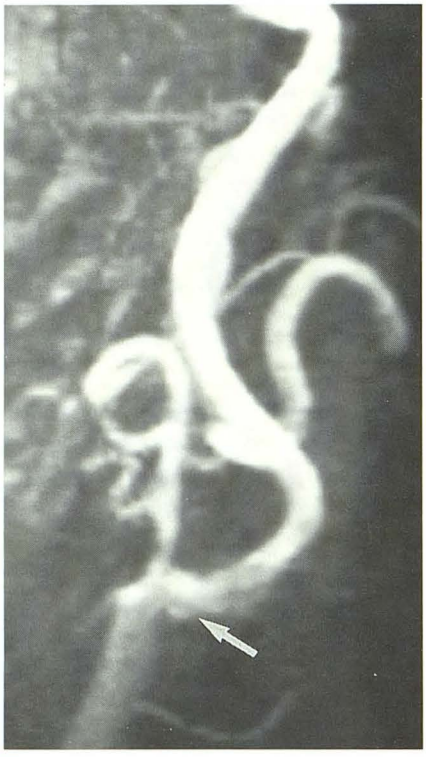

B

Fig. 10. Overestimation of stenosis by US resulting from tortuous vessel.

A, Longitudinal color-coded sonogram of ICA shows spectral broadening, which was interpreted as severe stenosis. No ulceration is detected.

This finding was anticipated by the effect of turbulent flow on intravoxel phase dispersion, which leads to signal loss. Critical stenoses on XRA corresponded to sites on MRA at which the vessel lumen narrowed to a thread (Fig. 9), or disappeared completely but was seen again a short distance beyond the presumed stenosis (Fig. 2). An occlusion on XRA corresponded to sites on MRA at which the vessel disappeared and was not seen beyond the stenosis.

US was relatively insensitive to low-grade stenosis; many vessels called mildly stenotic by MRA were described as normal by US.

For cases in which there was a greater than one grade difference in ICA stenosis assignment, the three modalities were inspected again to decide which modality was in error. In one case, a stenosis called moderate on US was critical on MRA and severe on XRA. This vessel also had a 50% stenosis at the origin of the CCA, which may have attenuated its velocity. A second case was called severe on US, but mild on MRA and XRA. The ICA of this vessel originated at an angle perpendicular to the CCA, which may have given rise to some spectral broadening (Fig. 10). A third case was classified as severe by US and mild by MRA. This patient had occlusion of the contralateral vessel, which may have resulted in compensatory flow and elevated velocities on the US study. A fourth case was critical on XRA, severe on MRA, but called normal by US, because the bifurcation was too high in the neck to be properly identified (Fig. 11). The bifurcation was also too high in a fifth case called moderate on US, severe on XRA and critical on MRA. A sixth case was called moderate by MRA, severe by XRA, and critical by US. The MR was of marginal quality due to patient jaw motion. The stenosis was mistakenly thought to be motion artifact. A seventh case was called normal by MRA, but severe on US. This case was collected early in the series, when a larger voxel size was in use. The MRA resolution was inadequate. In an eighth case, an ulcer at the same level as a severe stenosis was mistaken for a moderately stenotic lumen on MRA. The ulcer made the lumen appear wider. In a ninth case, a severe stenosis was missed on XRA because the lesion was obscured by the ECA.

B, Sagittal 3D TOF angiogram shows only mild stenosis. Ulceration of bulb is noted (*arrow*). These findings were in agreement with XRA. In retrospect elevated velocities encountered by Doppler resulted from sharp angle at which ICA originates from CCA.

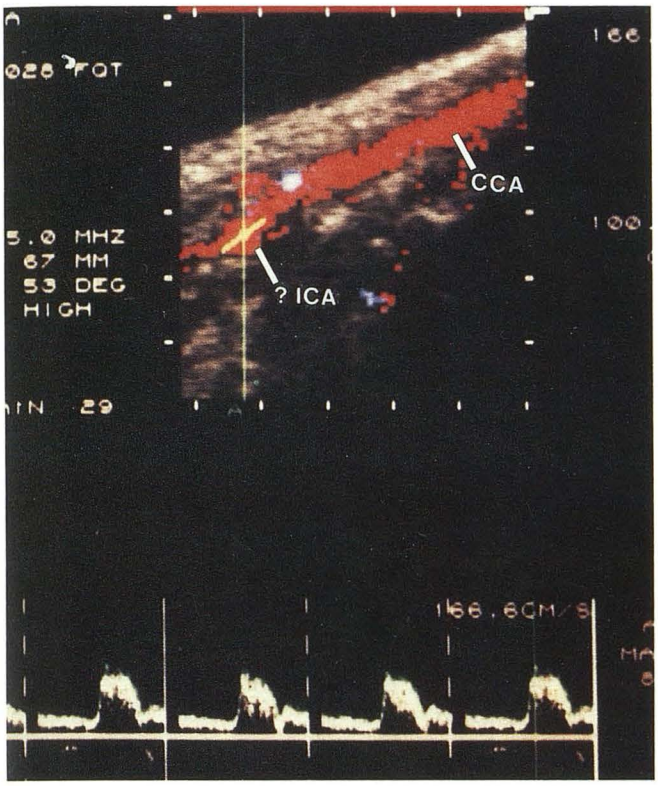

A

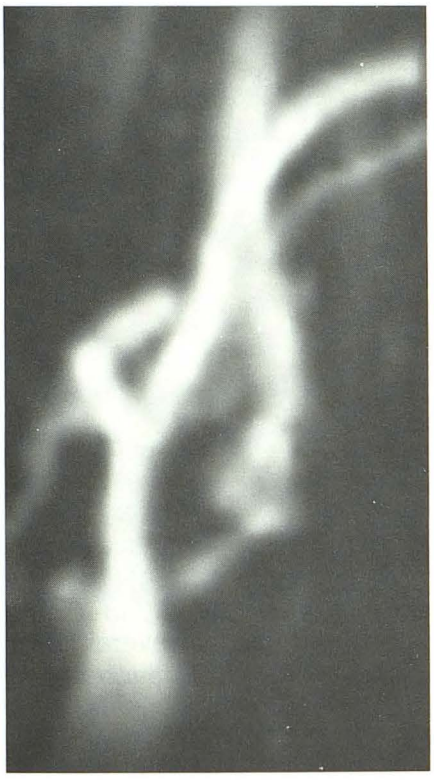

B

Fig. 11. Misidentification of ICA and ECA on US.
A, Sonogram shows normal flow in presumed proximal ICA. *B*, MRA demonstrates large ECA and critical stenosis of ICA. High bifurcation of carotid prevented recognition of branch vessels and identification of ECA on sonogram.

Two discrepancies could not be explained. A long, mild stenosis on MRA and XRA was called severe on US. Also a lesion called mild on XRA and moderate on MRA with a visible plaque was interpreted as normal on an apparently technically adequate US. Perhaps the bulb was sufficiently capacious so that a 50% stenosis did not elevate blood velocities.

Vessel Wall Depiction

In most cases, plaque could be visualized on single partitions of the sagittal 3D TOF acquisition. Plaque varied in intensity from gray to black. The significance of plaque intensity is uncertain, but in view of the prevalence of hemorrhagic plaque, the dark appearance could have resulted from heme products. MRA did not have sufficient resolution to assess the endothelial layer, or even to differentiate the layers of the arterial wall. It could resolve gray plaque from the dark muscular wall of the artery.

A 2-cm aneurysm of the proximal ICA in one individual was noted on US and on single slices of the MRA, but not on XRA. The aneurysm was partially thrombosed so that the lumen was normal in caliber.

Ulcers were rarely visualized on US. Focal concavities of the vessel wall seen on XRA were interpreted as ulcers, however, without histologic proof, it was difficult to know if these were truly ulcers with endothelial disruption or merely irregularly shaped plaques. Out of 16 concavities of the vessel wall that might have been ulcers by XRA, 11 were seen by MRA. Of those missed by MRA, three were 2 mm or less in diameter. One ulcer was encountered early in the series when thicker partitions were used on MRA. This may have led to a loss in contrast.

Study of Inter-Reader Variability

When 40 XRAs of good quality were independently graded by four readers, the Spearman correlations between the readers for both ICA and ECA origins ranged between 0.86 and 0.92 with a mean of 0.89, and for ICA origins only ranged between 0.90 and 0.96 with a mean of 0.93. There were no assignments more than one grade apart. The correlation was not 1.0 because fre-

quently lesions that were near the boundary between two grades could be put in either category. This observation involves different readers interpreting the same examinations, but it suggests that a panel of readers interpreting MRA and XRA would also produce a less than perfect correlation even if both sets of studies were free of technical deficiencies and artifacts. The correlations between MRA and XRA for the panel readers, 0.85 for ICAs and ECAs and 0.94 for ICAs only, are close to these means.

Discussion

Comparison of Stenosis Grades

Under the conditions of this study US, XRA, and MRA provided very similar assessments of the carotid bifurcation. The information in XRA and MRA was largely redundant for grading stenotic disease. In those cases in which MRA and XRA disagreed, MRA tended to overestimate the stenosis by one grade. This overestimation was due to intravoxel phase dispersion in areas of turbulent blood flow. Phase dispersion is minimized by the use of shorter echo times and smaller voxels. In this study, a TE of 7 msec and a voxel size of 0.86 × 0.86 × 1.0 mm was employed. It is likely that sequences with even smaller echo times and FOVs will be available in the future.

Among the discrepancies in ICA origin stenosis of more than one grade, five were the result of unrecognized artifacts in velocity on US, two of high carotid bifurcations on US, one of a poor choice of acquisition parameters on MRA, one of patient motion on MRA, one of an unrecognized ulcer on MRA, and one of insufficient views on XRA.

Dedicated Carotid Coil

Conventional head coils often do not extend caudally enough to visualize the carotid bifurcation. This is particularly a problem in patients with high shoulders. Neck imaging coils may be positioned as low as the carotid origins but they only receive signal, while relying on transmission of radio frequency pulses by the body coil. This results in saturation of thoracic blood, and, therefore, a loss of contrast, when neck coils are used for sagittal 3D TOF acquisition. For that reason, neck coils are generally used in conjunction with transverse sequential 2D, or transverse 3D TOF acquisition.

In this study a specially built transmit-receive carotid coil that could be positioned as low as the sternum allowed visualization of low bifurcations (Fig. 12). Although the intent of this investigation was to evaluate the bifurcation only, often the origins of the vertebral arteries and the right carotid artery could be seen on sagittal angiograms. The left carotid and brachiocephalic arteries originated too medially to be seen in the sagittal double-slab acquisition, necessitating an additional coronal 3D sequence to evaluate the carotid and brachiocephalic origins.

MRA Protocol

The MRA protocol selected here was sufficiently elaborate that it was usually scheduled as a separate procedure. It required 35 minutes of time in the magnet, and an additional 15 minutes of postprocessing and photography to complete the study. MIPs of each study were calculated before the patient left the magnet to determine whether additional acquisitions were necessary. Each of the three acquisitions contributed complementary information. 2D TOF was sensitive to slow flow, while 3D TOF displayed high resolution and freedom from in-plane saturation. If a lesion was detected on all three acquisitions, the readers felt that they could assign a stenosis grade with a high degree of confidence.

Patients could generally tolerate an additional T2-weighted spin-echo image of the brain to screen for prior stroke, or a siphon and circle-of-Willis MRA, or an aortic arch MRA, but not all of these studies in one session.

Comparison with Other Investigations

The results of clinical trials of the accuracy of MRA are likely to be dependent on the specific instrument used. Software implementation, shielding of gradients, and the availability of short echo times and small voxel volumes may have a strong influence on the quality of TOF images.

Our method differed in several respects with that of Litt et al (5). Litt favored MIP images without interpreting the individual slices, while we interpreted both individual slices and MIPs together. This strategy allowed us to directly visualize plaque. Litt used 2D TOF exclusively, while we used both 2D and 3D methods. The authors reported that about 70% of occluded ICAs were misclassified as severe or critically stenotic. They suggested this might have been due to external

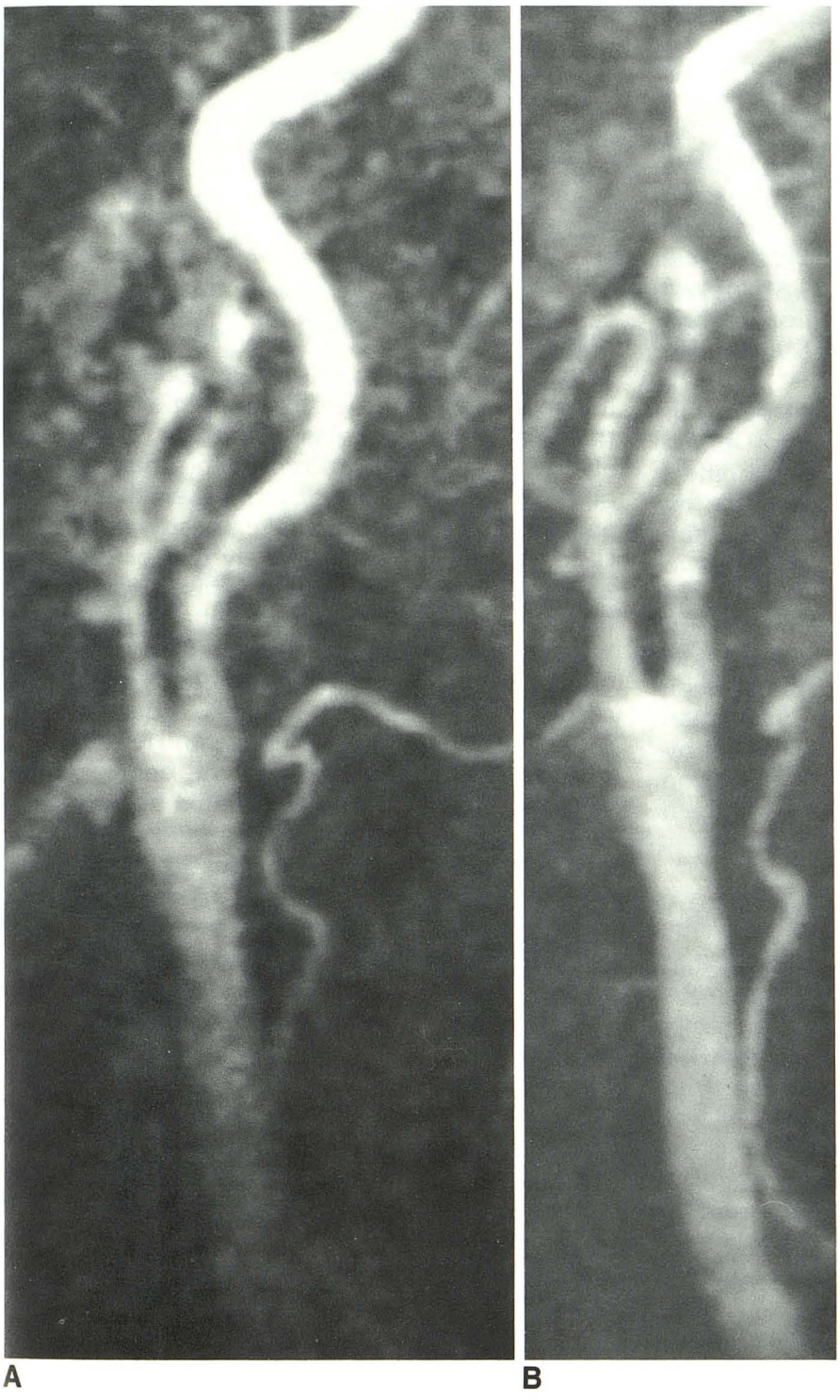

Fig. 12. Improved depiction of the carotid bifurcation using a dedicated carotid coil.

A, Sagittal 3D TOF angiogram of carotid bifurcation with the head coil. Bifurcation is low in neck. It falls outside of homogeneous volume of head coil resulting in poor sensitivity and small excitation flip angles.

B, Dedicated carotid coil may be positioned more caudal on neck, permitting image with greater signal-to-noise ratio.

or collateral branches that were mistaken for the ICA. In our protocol, we were able to make conclusive identification of the ICA by tracing it into the petrous bone on transverse 2D and sagittal 3D images, and conclusive identification of the ECA by visualizing extracranial branch vessels. Our images were collected with shorter echo times (7–10 msec vs 14–22 msec) and smaller voxels (.82 × .82 × 1.0 vs 1.37 × .98 × 2.5), which should have reduced intravoxel phase dispersion. There is a mild bias toward overestimation of stenosis grades in Litt's data, however, the generally good agreement between the modalities suggests that the readers were able to

take phase dispersion into account when interpreting their images.

Kido et al (6) evaluated 60 carotid bifurcations by XRA, and by 2D TOF MRA. They also used a projection phase contrast MRA technique (14). The authors concluded that it was useful to have two acquisitions available to provide complementary information. Four arteries were excluded from the study because the readers were unable to distinguish the ICA from the ECA. In two included cases, the readers misidentified the ICA and ECA. These errors might have been avoided with the use of 3D TOF sequences.

Masaryk et al (7) collected sagittal 3D TOF angiograms only and compared them to DSA in 65 bifurcations. They found no statistical difference between the average stenosis measured by MRA and DSA. They computed a Spearman correlation of 0.95 and 0.97 between the two methods for assessment of percent stenosis of the left and right carotid bifurcations, respectively. The authors noted that tortuous vessels left the volume of the sagittal slab. In our protocol, this problem is detected by a MIP calculation after the sagittal acquisition, and is remedied by an additional transverse 3D slab acquisition through the bifurcation or area of suspected stenosis.

Relative Strengths of Carotid Imaging Modalities

In this study, MRA exhibited capabilities that were similar to both US and XRA. Like US, MRA was noninvasive and did not require contrast injection. It could visualize plaque. Like XRA, MRA images could be read retrospectively with little operator dependence. With adequate choice of sequences, the reader was unlikely to mistake the ECA for the ICA, or to become confused by tortuous or collateral vessels. It could visualize the carotid artery from the arch to the siphons (8), although this capability was not evaluated in the current study.

Unlike US or XRA, viewing orientations could be chosen after the examination was completed.

MRA failed when patients were claustrophobic, could not remain motionless, or had hemostatic clips in the vicinity of the carotid artery. It was not affected by factors that may compromise XRA (ie, poor renal function, contrast reaction, coagulopathy, lack of femoral pulses, inability to advance catheter), or US (tortuous vessels, unfavorable location of lesion, thick mural calcifications, immediately post-op from endarterectomy). In that sense, the examinations were complementary.

A subject for further investigation would be to compare plaque morphology as determined by MRA, US, and examination of the surgically resected specimen.

Potential Role of MRA

The question of whether MRA will compete primarily with US as a screening exam or with XRA as an anatomic exam is important because it directs one to develop either MRA protocols that feature quick acquisition times, or high reliability and resolution. Considering that the cost of MRA may be twice or more than that of US, and that many surgeons have already invested in US equipment, MRA is unlikely to replace US as a carotid screening modality. This is particularly true in asymptomatic or low-probability patients.

If additional investigations confirm the results of this study, namely that MRA and XRA provide redundant information, then the goal of MRA should be to replace the expense and risk of XRA. To accomplish this, MRA of the entire carotid from the arch to the siphons could be combined with imaging of brain parenchyma to detect prior stroke, in one or two imaging sessions. Given the goal of providing a definitive angiographic exam, the use of an extended MRA protocol, such as the one in this study, is justified.

References

1. Laub GA, Kaiser WA. MR angiography with gradient motion refocusing. *J Comput Assist Tomogr* 1988;12:377–382
2. Lenz GW. *Advances in time-of-flight MR angiography*. Paper presented at the Society of Magnetic Resonance Imaging, Chicago, April 1991
3. Schmalbrock P, Yuan C, Chakeres DW. Volume MR angiography: methods to achieve very short echo times. *Radiology* 1990;175:861–865
4. Gullberg GT, Wehrli FW, Shimakawa A, et al. MR vascular imaging with a fast gradient refocusing pulse sequence and reformatted images from transaxial sections. *Radiology* 1987;165:241–246
5. Litt AW, Eidelman EM, Pinto RS, et al. Diagnosis of carotid artery stenosis: comparison of 2DFT time-of-flight MR angiography with contrast angiography in 50 patients. *AJNR* 1991;12:149–154
6. Kido DK, Panzer RJ, Szumowski J, et al. Clinical evaluation of stenosis of the carotid bifurcation with magnetic resonance angiographic techniques. *Arch Neurol* 1991;48:484–489
7. Masaryk AM, Ross JS, DiCello MC, et al. 3DFT MR angiography of the carotid bifurcation: potential and limitations as a screening examination. *Radiology* 1991;179:797–804
8. Anderson CM, Saloner D, Lee RE, et al. Dedicated coil for carotid MR

angiography. *Radiology* 1990;176:868–872
9. Masaryk AM, Modic MT, Ruggiere PM, et al. Three-dimensional (volume) gradient-echo imaging of the carotid bifurcation: preliminary clinical experience. *Radiology* 1989;171:801–806
10. Rossnick SG, Laub GA, Braeckle R. Three dimensional display of blood vessels. In: *Proceedings of the IEEE Computers in Cardiology Conference*. New York: Institute of Electrical and Electronic Engineers, December 1986:193–196
11. Anderson CM, Saloner D, Tsuruda JS, et al. Artifacts in maximum-intensity-projection display of MR angiograms. *AJR* 1990;154:623–629
12. Bluth EI, Stavros AT, Marich KW, et al. Carotid duplex sonography: a multicenter recommendation for standardized imaging and Doppler criteria. *Radiographics* 1988;8:487–506
13. Noether GE. *Introduction to statistics the nonparametric way*. New York: Springer-Verlag, 1991:236
14. Dumoulin CL, Hart HR Jr. Magnetic resonance angiography. *Radiology* 1986;161:717–720

Please see the Commentary by Ackerman and Candia on page 1005 in this issue.